



Microstructure and mechanical properties of 7075 aluminum alloy during complex thixoextrusion

Jian LIU¹, Yuan-sheng CHENG¹, Sin Wing Norman CHAN², Daniel SUNG²

1. National Key Laboratory for Precision Hot Processing of Metal, Harbin Institute of Technology, Harbin 150001, China;
2. KaShui Technology (Huizhou) Co., Ltd., Huizhou 516000, China

Received 15 March 2020; accepted 10 September 2020

Abstract: 7075 aluminum alloy was used to obtain elbow parts by complex thixoextrusion and the microstructure evolution and mechanical properties during this process were studied by SEM, TEM and other analytical methods. The results show that different parts in 7075 aluminum alloy show quite different microstructures. The microstructure of the thin walls formed by back-extrusion is stratified, and the bottom of the parts formed by angular extrusion is obviously deformed. Shear forces contribute to the crushing of grains and the coarse second phase. The main strengthening phases in the material are η phase and E phase, whose amounts greatly decrease during heating to semi-solid and thixoextrusion. After heat treatment, they can precipitate evenly to improve the mechanical properties of the material. The average tensile strength of whole part after thixoextrusion and heat treatment is 485.49 MPa, while the average elongation is 5.49%.

Key words: 7075 aluminum alloy; thixoextrusion; semi-solid forming; elbow parts; mechanical properties

1 Introduction

7075 aluminum alloy is a precipitation-hardened alloy, with high specific strength and specific stiffness, good fracture toughness and corrosion resistance, and excellent molding performance, belonging to super-high strength deformation aluminum alloy [1–5]. It is one of the vital structural materials in aerospace and transportation industry, whose properties are affected by metal compound particles, solid solution particles, grain structure and dislocation [6,7]. Especially after the proper solution and aging treatment, its performance can be changed obviously [8,9].

Semi-solid metal forming/processing (SSF or SSP) is a metal forming process that takes advantage of the good rheological properties of metals in the semi-solid zone [10,11]. Thixoforming

is an important way of semi-solid forming and a plastic deformation method that can form complex parts. Therefore, this method is mainly used in experiments and industrial production [12–14]. GABRIELA et al [15] proposed a method to process DSC curves using the principles of calculus to identify the critical temperature in thixoextrusion formability analysis. CHEN et al [16] used strain-induced melting activation (SIMA) to prepare 7075 aluminum alloy billets and then used the semi-solid thixotropic forging technology to form a certain brand of end cover parts for vehicles, which had good structural integrity and mechanical properties. YANG et al [17] pressed two kinds of alloys simultaneously in semi-solid state into the same forging cavity. Then, the bimetallic composites composed of Sn–15%Pb and Pb–22%Sn alloy were formed by using thixotropic forging. The results showed that the composite interface was well

organized. ARIF et al [18] used the thixoforming method to study the influence of Cu and Mg on the thixoforming and mechanical properties of 2014 aluminum alloy. The experimental results showed that the solidification interval temperature of the alloy could be reduced by reducing Cu content. The formation of dense π -Al₈FeMg₃Si₆ phase could be promoted by increasing the magnesium content. Thus the strength of alloy was improved. In general, in the current studies on thixoforming, the thixoformed parts are relatively simple and the deformation direction is single. More attention has been paid to the development of new materials. For extrusion, the deformation direction is single and the material flow is simple, and there is no great difference in the microstructure and properties of the parts [19,20]. Studies have shown that extrusion can change the granular grain structure of semi-solid 7075 aluminum alloy into deformed fiber structure and may affect the second phase [21–26]. However, there is less detailed analysis on the microstructure evolution and mechanical properties of 7075 aluminum alloy during complex thixoextrusion worldwide, which is of great research significance.

In this work, the microstructure evolution and mechanical properties of 7075 aluminum alloy during the thixoextrusion process of forming elbow

parts were studied. The deformation of 7075 aluminum alloy was very complex, involving upsetting, reverse extrusion, and bending angle extrusion. This research can not only guide industrial production, but also help to understand the regional differences of bulk semi-solid aluminum alloys under different deformation conditions.

2 Experimental

2.1 Materials

SIMA was used to prepare the semi-solid billet. The billet in this experiment was composed of 7075 aluminum alloy, with chemical composition given in Table 1.

Table 1 Chemical composition of 7075 aluminum alloy raw material (wt.%)

Cu	Zn	Mg	Fe	Cr	Mn	Si	Al
1.56	6.0	2.3	0.03	0.17	0.27	0.26	Bal.

2.2 Thixoextrusion and heat treatment process

The billet was 85 mm in height and 90 mm in diameter, as shown in Fig. 1(a). The billet was formed by thixoextrusion with the mold shown in Fig. 1(b), and the elbow parts shown in Figs. 1(c, d)

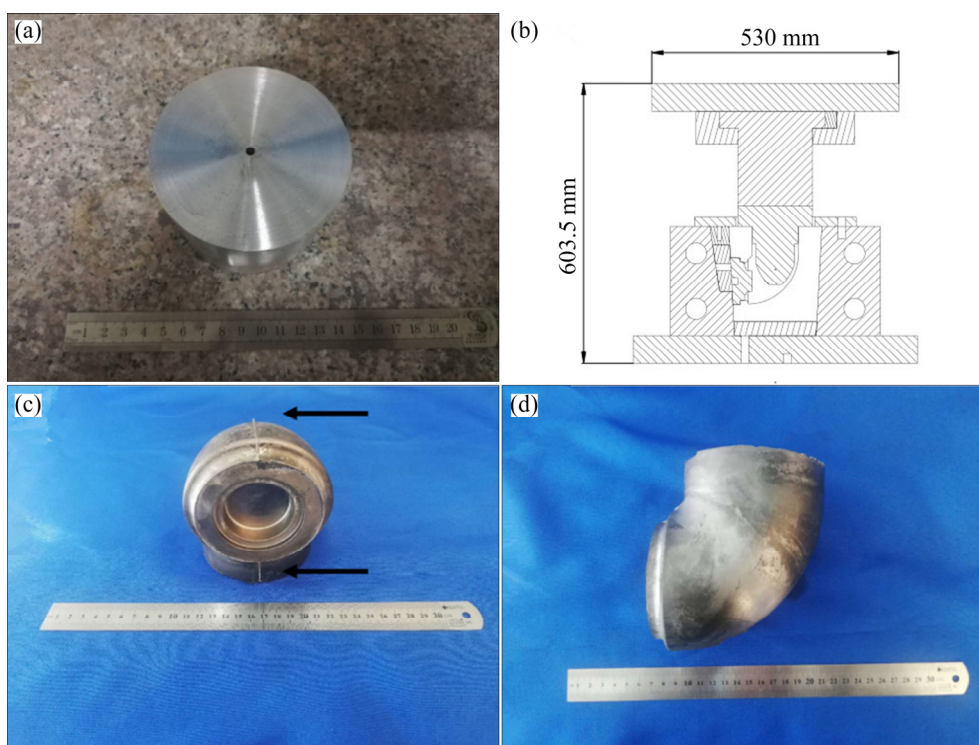


Fig. 1 Billet (a), mold (b) and 7075 aluminum alloy elbow parts after thixoextrusion (c, d)

were obtained. The isothermal treatment temperature of billet was 610 °C, the forming temperature was 590 °C, and the mold temperature was 280–320 °C. Furthermore, the heat treatment schedule was 8 h for solution at 460 °C and 24 h for aging at 105 °C.

2.3 Microstructure and mechanical property analysis

Samples used for metallographic observation and scanning electron microscopy (SEM) were polished and corroded with Keller solution. The samples used for transmission electron microscopy (TEM) analysis were polished and thinned to less than 50 μm, which could be used for experiment after ion thinning by Gatan Model 691 precision ion thinning instrument. Tensile tests were carried out on the universal material testing machine (AG-Xplus50kn) to determine the mechanical properties of the material such as tensile strength and elongation.

3 Results

3.1 Microstructure of 7075 aluminum alloy during complex thixoextrusion

In order to analyze the microstructure, billet samples were cut from the tube wall at 5 positions of the top part, the bending part, the middle part, the prominent part and the bottom of the elbow parts, as shown in Fig. 2.

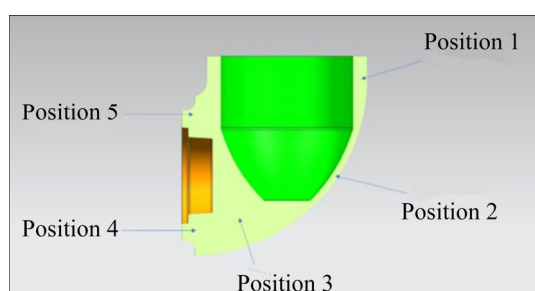


Fig. 2 Schematic diagram of sampling positions of thixoextruded part

Figure 3 shows the metallographic images of the thixoextruded parts at Positions 1–5. At Position 1, it can be seen that two different microstructures are layered. The morphology of the upper layer is mostly similar to that of the as-cast structure, in which spherical grains are dispersed and the diameter of the coarse grains is about 150 μm. The lower layer is of the semi-solid structure without

deformation, and the grain boundary is obvious. The grain size is about 150 μm, and the grain deformation is very small, basically maintaining the sphericity. The reason is that after isothermal treatment, a large amount of liquid phases appear in the semi-solid billet, and most of the liquid *E* phase exists at the grain boundary. Driven by the liquid phase, a small part of the grains surrounded by the liquid phase flow in the opposite direction of extrusion and finally solidify. As can be seen from Fig. 3(a), the grains in the upper layer are mostly long in transverse direction and short in longitudinal direction. The morphology of the grains in the lower layer shows the opposite phenomenon, which indicates that the grains are mainly affected by the tensile stress caused by the contact between the die and the blank during the forming process.

Obvious plastic deformation characteristics can be seen from the microstructure of Position 2. The original coarse spherical grains are elongated and broken along the deformation direction, and the isoaxial crystals with a diameter of 10–20 μm, formed by dynamic recrystallization, are evenly distributed in the billet, resulting in the work hardening. There is little liquid phase at the grain boundary. Due to the friction between the die and the billet, the curved passage acts as an equal-diameter angular extrusion to shear the billet. The grains here are more fragmented and recrystallized fully, so the grains are smaller than those in other locations. The black spots in Fig. 3(b) are coarse and broken second phase particles, which are uniformly distributed in the matrix instead of agglomerating. The microstructures of Position 3 and Position 4 are similar. The larger spherical shape of grains can also be observed and the smaller recrystallized grains can be clearly seen. The deformation is mainly caused by forward extrusion. The deformation of this part is small relatively, so the recrystallization is not as sufficient as that at Position 2. The microstructure of Position 5 shows large spherical grains, and the liquid phase is obvious at the grain boundary. However, a small amount of recrystallized grains can also be found.

3.2 Mechanical properties of 7075 aluminum alloy during complex thixoextrusion

The mechanical properties of 7075 aluminum alloy can be greatly enhanced by heat treatment.

Figure 4 shows the sampling positions of the tensile-testing specimen at room temperature.

The differences of mechanical properties before and after heat treatment are compared, and the histogram is drawn in Fig. 5. It can be seen that the average tensile strengths before and after heat

treatment are 276.16 and 485.49 MPa, respectively. The highest value is 510.76 MPa, and the average tensile strength after heat treatment is 75.7% higher than that before heat treatment. After aging, the elongation of the material is improved greatly. The average elongation before heat treatment is 2.99%,

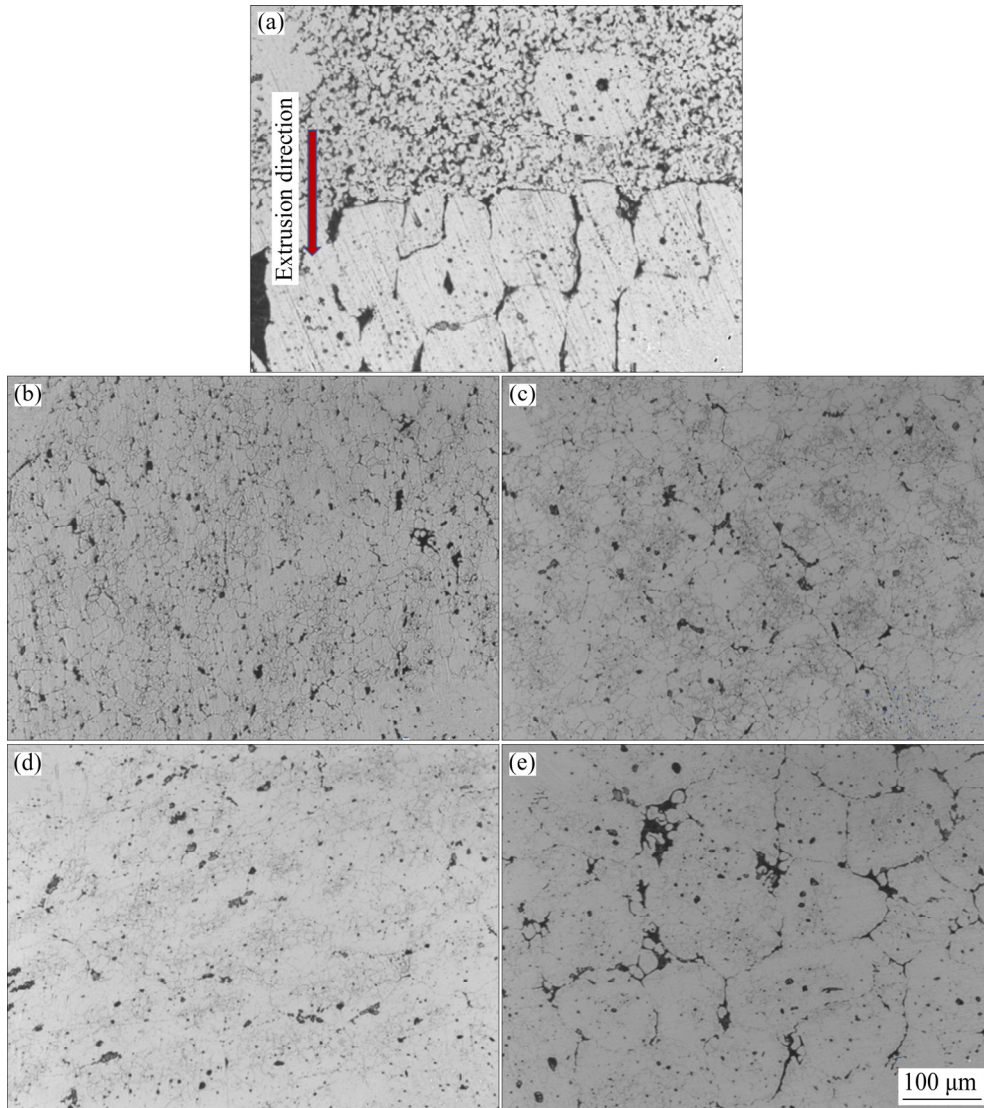


Fig. 3 Metallographic images of thixoextruded part at different positions: (a) Position 1; (b) Position 2; (c) Position 3; (d) Position 4; (e) Position 5

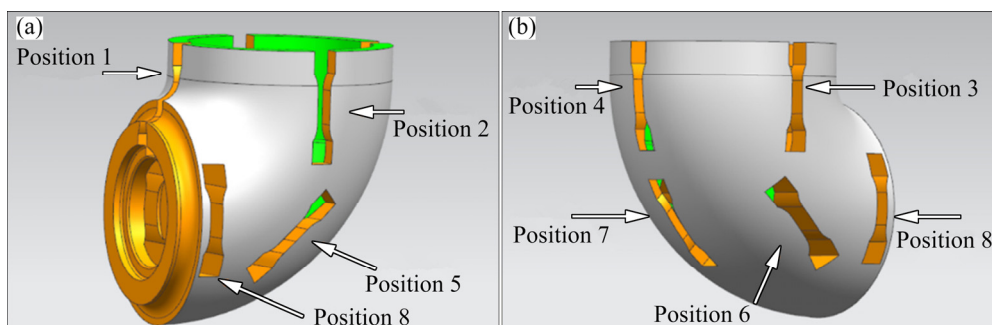


Fig. 4 Sampling positions of thixoextruded parts for tensile testing

while the average elongation after heat treatment is 5.49%, and the maximum elongation is 7.99%. Most of the positions with the low tensile strength are at the reverse extrusion wall, which are Positions 1–4. The reason is that there are many liquid phases in the upper part of the part. The grain size is large, and there is no recrystallization. The appearance of layered structure leads to the mechanical properties of this part to decline significantly. The tensile strength of Position 7 is always the maximum. Because of the shear action of the curved channel, the grains here are smaller

and the distribution of the second phase is more uniform.

4 Discussion

4.1 Second phase of 7075 aluminum alloy before complex thixoextrusion

After complex thixoextrusion, the morphology and distribution of the second phase of 7075 aluminum alloy can greatly affect the properties of the material [27]. Figure 6 shows the typical second phase distribution and elemental analysis results of

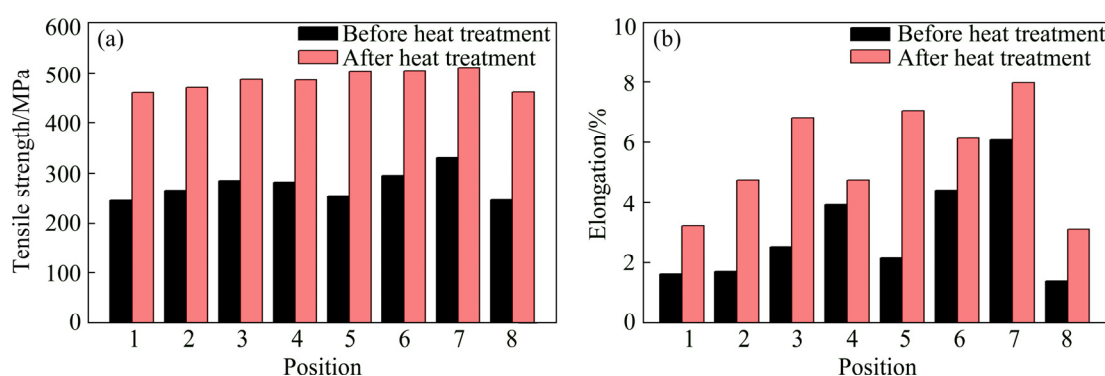


Fig. 5 Tensile strength (a) and elongation (b) of thixoextruded part before and after heat treatment

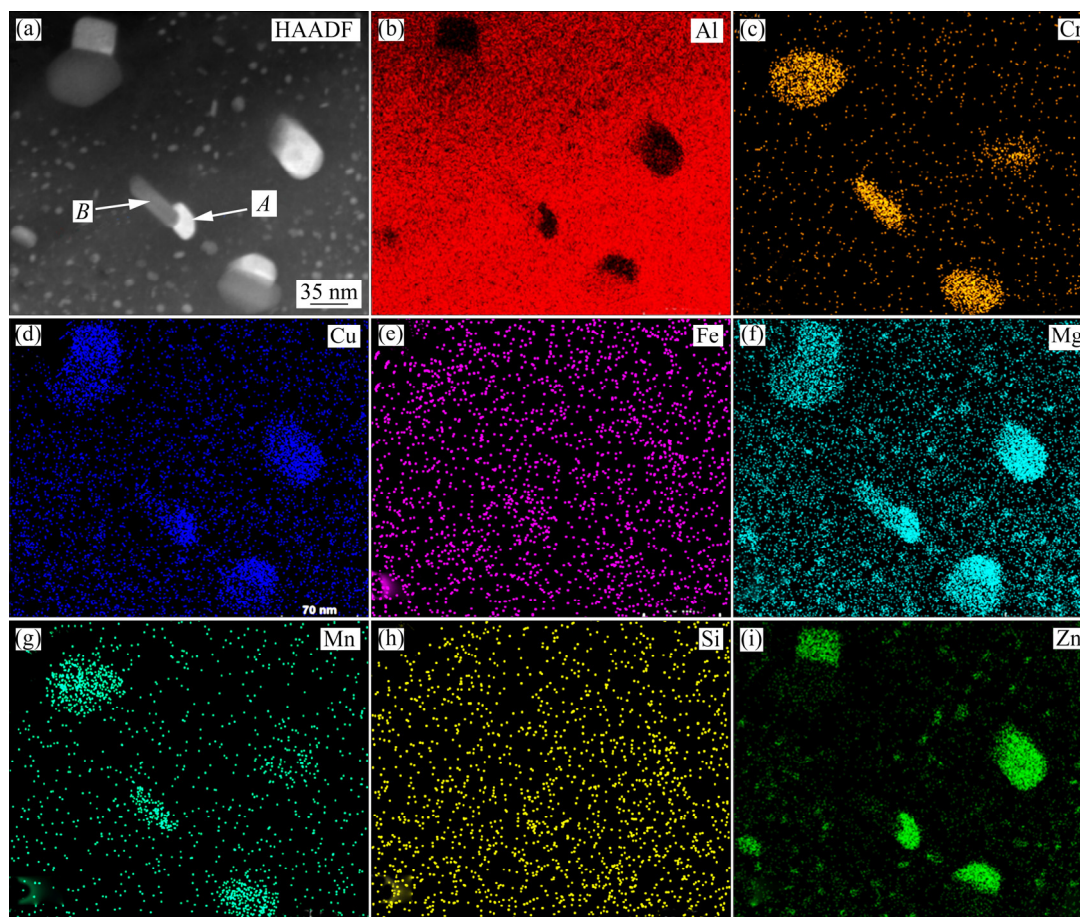


Fig. 6 TEM image (a) and elemental analysis results (b–i) of 7075 aluminum alloy raw material

raw materials. It can be seen that the fine precipitated phase mainly contains Mg and Zn elements, which is speculated to be equilibrium η phase (MgZn_2). Among the precipitated η phases, the second phase with a size of about 50 nm is dispersed. It consists of two parts: one is the brighter second phase indicated by Arrow A in Fig. 6(a), which is inferred to be the thick η phase according to the distribution of elements; the other is the darker second phase indicated by Arrow B, containing elements Al, Mg and Cr, which is speculated to be E phase ($\text{Al}_{18}\text{Mg}_3\text{Cr}_2$). Harmful elements such as Fe and Si do not appear in the dispersed and precipitated phase, indicating that the elements such as Fe and Si mainly harm the material properties by forming the continuous second phase with large size at the grain boundary. As η phase nucleates in the E phase, it absorbs the surrounding elements of Mg and Zn. As a result, there are not enough Mg and Zn elements in the surrounding matrix for nucleation growth, leading to the emergence of precipitation free zone.

Figure 7 shows high-resolution TEM morphology of the second phase and the corresponding selected electron diffraction pattern.

It can be seen that the second phase presented as a bar is about 50 nm in size. By calibrating the selected electron diffraction spots, it can be determined that the second phase presented as a bar at Position A is E phase, while the second phase attached to E phase at Position B is η phase. Since E phase is not coherent with $\alpha(\text{Al})$ matrix, and the specific volume of E phase is different from that of $\alpha(\text{Al})$ matrix, resulting in the increase of elastic strain energy, there are higher interface energy and elastic strain energy at the interface of E phase and $\alpha(\text{Al})$ matrix. During the non-uniform nucleation of η phase, the release of interface energy and elastic strain energy here can reduce nucleation work. Therefore, the interface between E phase and $\alpha(\text{Al})$ matrix is one of the typical locations of non-uniform nucleation of η phase [28–30].

4.2 Second phase of 7075 aluminum alloy after complex thixoextrusion

Figure 8 shows the bright field TEM images of the raw material and the material after thixoextrusion. Compared with the raw material, the amount of E phase in 7075 aluminum alloy after thixoextrusion is significantly reduced,

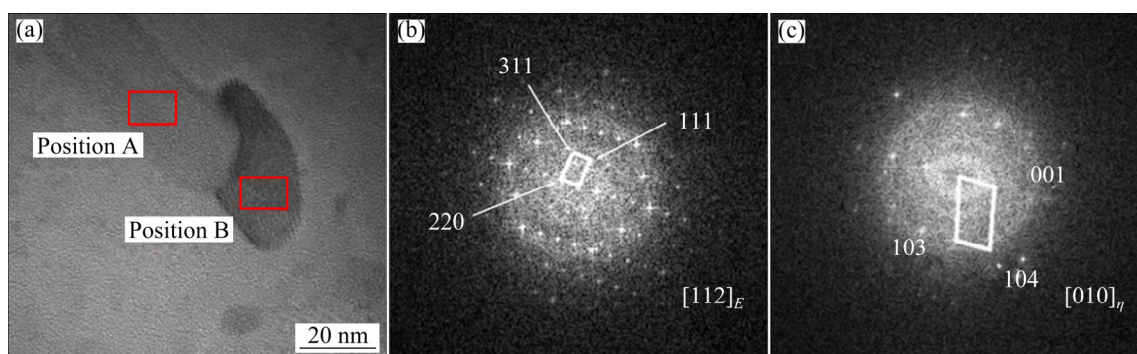


Fig. 7 High resolution TEM photograph of second phase (a) and selective electron diffraction patterns at Position A (b) and Position B (c)

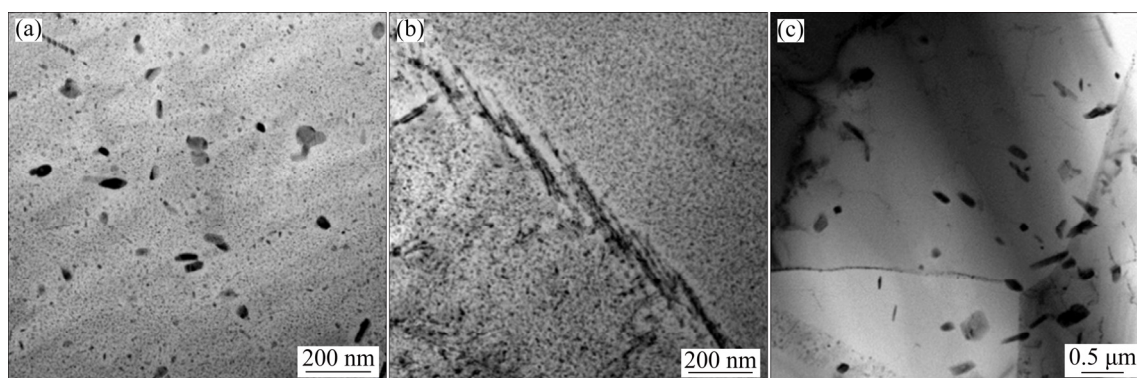


Fig. 8 Bright field TEM images of 7075 aluminum alloy raw material (a) and thixoextruded parts (b, c)

indicating that E phase is dissolved into matrix or grain boundary during heating the billet to semisolid state. Since E phase is formed during the homogenization process, it will appear again in large quantities after solution treatment. Figure 8(c) shows that the size of the second phase is around $500\text{ nm} \times 100\text{ nm}$ and it is enriched at the grain boundary. Two typical dispersed phases have a second phase morphology, with one in the form of a block and the other in the form of a rod. They play the role of pinning grain boundaries, which is beneficial to material properties.

Figure 9 shows the bright field TEM images of the block phase of 7075 aluminum alloy after thixoextrusion. From Fig. 9(a), it can be seen that two rods are embedded in the block-shaped second phase, which may be another second phase, or it may be caused by the change of crystal plane. As can be seen from Fig. 9(b), some point-like precipitated phases grow at the interface of the rod, which is typical for the nucleation growth of η

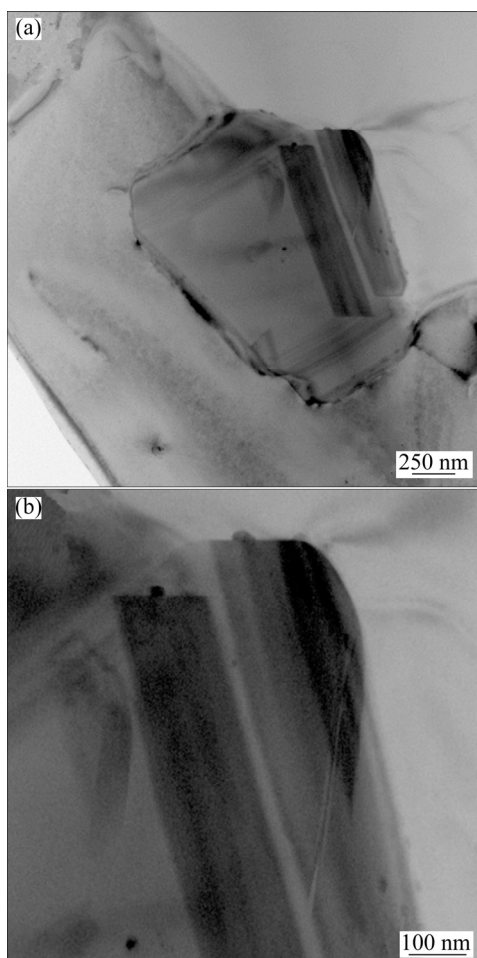


Fig. 9 Bright field TEM image of block phase of 7075 aluminum alloy after thixoextrusion

phase on E phase. Therefore, the bar is speculated to be E phase, the precipitated phase is speculated to be η phase, and the block phase should be a dispersive phase with a high melting point.

Figure 10 shows selected diffraction spots and high-resolution image of the dispersive phase. After calibration, it is determined to be Al_3Mn . The rhombic crystal system is (200) with a spacing of 0.726 nm while the spacing between the crystal planes of (143) is 0.269 nm . It is located at the grain boundary, and it is conducive to improving the mechanical properties of 7075 aluminum alloy.

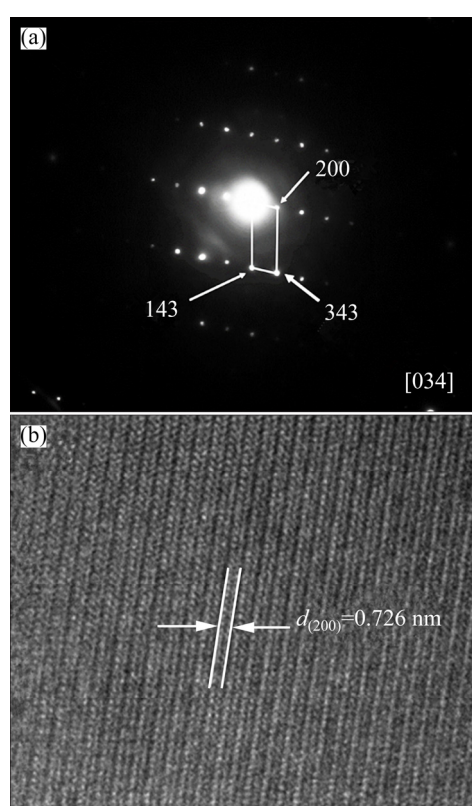


Fig. 10 Selection diffraction spots (a) and high resolution image (b) of dispersive phase

In order to understand the difference between block second phase and rod second phase components, the area scanning of the material is conducted, as shown in Fig. 11. It can be seen that the second phase is rich in Al, Mg, Zn, Cu, Cr and Mn, which are the main elements of the dispersive E phase and Al_3Mn . There is not much difference between the rod and block phases, which indicates that the two phases can grow together. It is also known that not all E phases dissolve into the matrix or grain boundary during heating the billet to semi-solid. Some grain boundaries are rich in Zn,

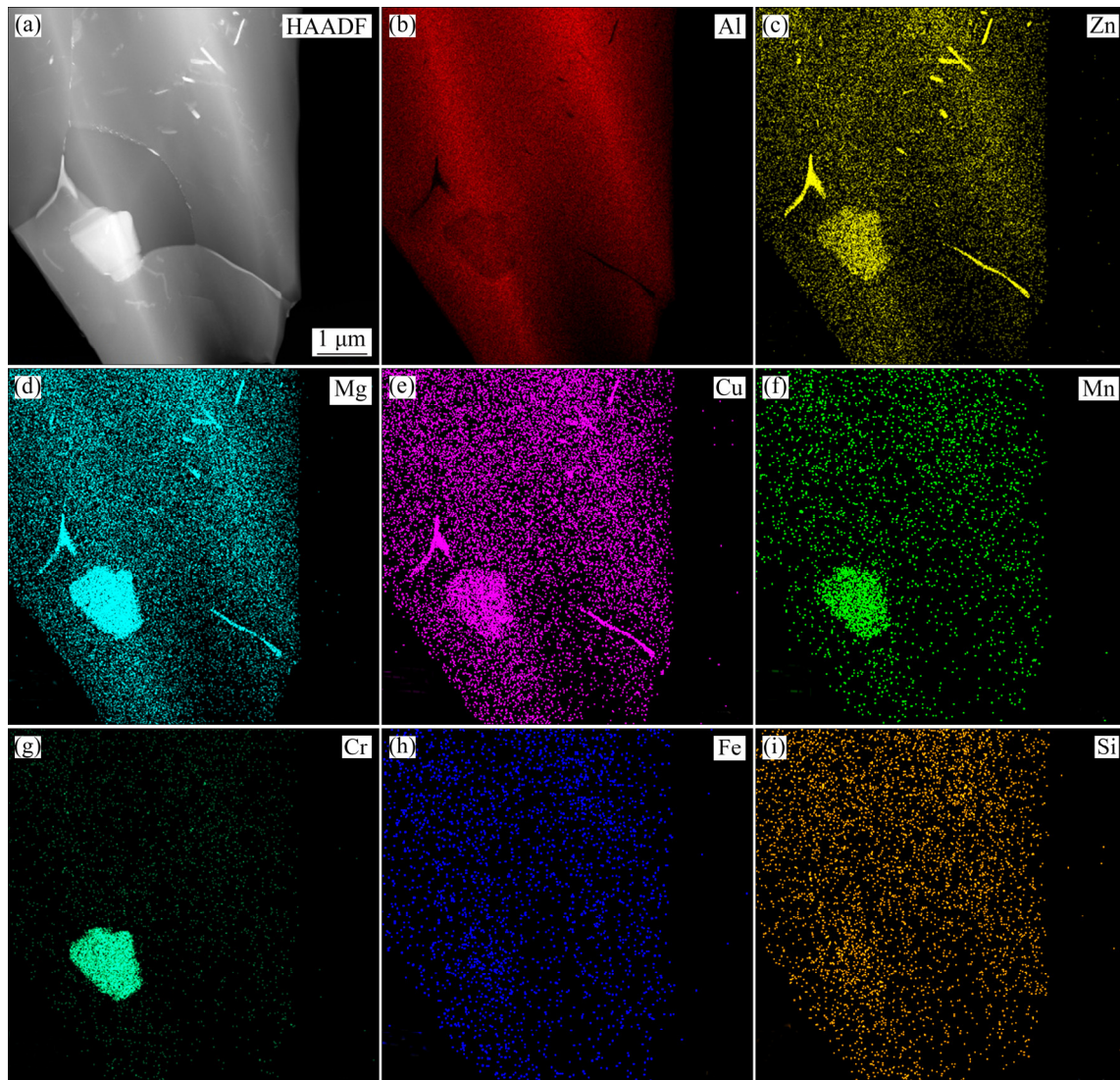


Fig. 11 Area scanning of dispersive second phase

Mg and Cu elements. These grain boundaries are broken and distributed in the matrix, which is caused by the plastic deformation of materials during extrusion.

5 Conclusions

(1) During the complex thixoextrusion, the microstructure of each part of 7075 aluminum alloy can be quite different. The existence of shear force contributes to the crushing of grain and the second phase, and the mechanical properties of the material can be greatly reduced.

(2) Elbow parts were obtained from semi-solid billet of 7075 aluminum alloy through thixoextrusion at 575 °C. After the heat treatment at 460 °C for 8 h and aging at 105 °C for 24 h, the

average tensile strength of the parts is 485.49 MPa, and the average elongation is 5.49%. The maximum tensile strength is 510.76 MPa and the maximum elongation is 7.99%.

(3) In the raw material of 7075 aluminum alloy, the η phase is evenly distributed in the matrix, while the E phase is widely distributed at the grain boundary and the η phase grows attached to the E phase. After heating to semi-solid and thixoextrusion, the η phase in 7075 aluminum alloy is dissolved into the matrix again, and the amount of E phase is greatly reduced. The partially undissolved E phase grows and co-grows with the second phase containing Mn. After heat treatment, the η phase and E phase gradually precipitate, and the mechanical properties of the material are improved.

References

- [1] TIAN F Q, LI N K, CUI J Z. Development process and direction of strengthening and toughening of ultra-high strength aluminum alloy [J]. *Light alloy Processing Technology*, 2005, 33(12): 1–9.
- [2] ZHOU Bing, LU Shuai, XU Kai-le, XU Chun, WANG Zhan-yong, WANG Bin-jun. Hot cracking tendency test and simulation of 7075 semi-solid aluminium alloy [J]. *Transactions of Nonferrous Metals Society of China*, 2020, 30(2): 318–332.
- [3] REN J, WANG R C, FENG Y, PENG C Q, CAI Z Y. Microstructure evolution and mechanical properties of an ultrahigh strength Al–Zn–Mg–Cu–Zr–Sc (7055) alloy processed by modified powder hot extrusion with post aging [J]. *Vacuum*, 2019, 161: 434–442.
- [4] GARCIA-INFANTA J M, ZHILYAEV A P, SHARAFUTDINOV A, RUANO O A, CARRENO F. An evidence of high strain rate superplasticity at intermediate homologous temperatures in an Al–Zn–Mg–Cu alloy processed by high-pressure torsion [J]. *Journal of Alloys and Compounds*, 2009, 473: 163–166.
- [5] HORITA Z, FUJINAMI T, NEMOTO M, LANGDON T G. Improvement of mechanical properties for Al alloys using equal-channel angular pressing [J]. *Journal of Materials Processing Technology*, 2001, 117: 288–292.
- [6] WILLIAMS J C, STARKE E A. Progress in structural materials for aerospace systems [J]. *Acta Materialia*, 2003, 51: 5775–5799.
- [7] JAVDANI A, DAEI-SORKHABI A H. Microstructural and mechanical behavior of blended powder semisolid formed Al7075/B₄C composites under different experimental conditions [J]. *Transactions of Nonferrous Metals Society of China*, 2018, 28(7): 1298–1310.
- [8] PHILLION A B, COCKCROFT S L, LEE P D. A three-phase simulation of the effect of microstructural features on semi-solid tensile deformation [J]. *Acta Materialia*, 2008, 56: 4328–4338.
- [9] ATKINSON H V, BURKE K, VANEETVELD G. Recrystallisation in the semi-solid state in 7075 aluminium alloy [J]. *Materials Science and Engineering A*, 2008, 490: 266–276.
- [10] LIN H Q, WANG J G, WANG H Y. Effect of predeformation on the globular grains in AZ91D alloy during strain induced melt activation (SIMA) process [J]. *Journal of Alloys and Compounds*, 2001, 431: 141–147.
- [11] SHEIKH-ANSARI M H, AGHAIE K M. Constitutive modeling of semisolid deformation for the assessment of dilatant shear bands [J]. *Applied Mathematical Modelling*, 2019, 70: 128–138.
- [12] WANG Yong-fei, ZHAO Sheng-dun, ZHANG Chen-yang. Microstructures and mechanical properties of semi-solid squeeze casting ZL104 connecting rod [J]. *Transactions of Nonferrous Metals Society of China*, 2018, 28(2): 235–243.
- [13] FAN Z. Semisolid metal processing [J]. *International Materials Reviews*, 2002, 47: 49–85.
- [14] CHEN Gang, ZHANG Yu-min, DU Zhi-ming. Mechanical behavior of Al–Zn–Mg–Cu alloy under tension in semi-solid state [J]. *Transactions of Nonferrous Metals Society of China*, 2016, 26(3): 643–648.
- [15] GABRIELA L B, CECILIA T W P, LEANDRO C P. An alternative method to identify critical temperatures for semisolid materials process applications using differentiation [J]. *Thermochimica Acta*, 2017, 615: 22–33.
- [16] CHEN Gang, CHEN Qiang, QIN Jin. Effect of compound loading on microstructures and mechanical properties of 7075 aluminum alloy after severe thixoformation [J]. *Journal of Materials Processing Technology*, 2016, 229: 467–474.
- [17] YANG Zhao, WU Ye-feng, ZHANG Wei, ZHOU Li. Study on preparation of Pb/Sn alloy bimetal composite products by thixo-forging [C]//Green Intelligent Casting Report. Casting Association, 2019: 76–79.
- [18] ARIF M A M, OMAR M Z, SAJURI Z, SALLEH M S. Effects of Cu and Mg on thixoformability and mechanical properties of aluminium alloy 2014 [J]. *Transactions of Nonferrous Metals Society of China*, 2020, 30(2): 275–287.
- [19] XIAO G F, JIANG J F, LIU Y Z, WANG Y, GUO B Y. Recrystallization and microstructure evolution of hot extruded 7075 aluminum alloy during semi-solid isothermal treatment [J]. *Materials Characterization*, 2019, 156: 109874.
- [20] YIN X L, DENG W J, ZOU Y H, ZHANG J Y. Ultrafine grained Al 7075 alloy fabricated by cryogenic temperature large strain extrusion machining combined with aging treatment [J]. *Materials Science and Engineering A*, 2019, 138106.
- [21] KILICLI V, AKAR N, ERDOGAN M, KOCATEPE K. Tensile fracture behavior of thixotropic cast AA7075 alloy [J]. *Transactions of Nonferrous Metals Society of China*, 2016, 26(5): 1222–1231.
- [22] TAHERI M M, ZAREI H A, ABEDI H R. Hot ductility behavior of an extruded 7075 aluminum alloy [J]. *Materials Science and Engineering A*, 2015, 637: 107–122.
- [23] DE AQUINO L, GUTIERREZ C E, ESTRADA G I, HINOJOSA R G, GARCIA S E, HERRERA R J M, PEREZ B R, MARTINEZ S R. Structural characterization of aluminium alloy 7075–graphite composites fabricated by mechanical alloying and hot extrusion [J]. *Materials and Design*, 2014, 53: 1104–1111.
- [24] ADRIANA N, VERONIQUE F, REGIS B, MARIANA P. Microstructure and flow behaviour during backward extrusion of semi-solid 7075 aluminium alloy [J]. *Journal of Materials Processing Technology*, 2012, 212: 1472–1480.
- [25] JAVDANI A, POUYAFAR V, AMEL A. Blended powder semisolid forming of Al7075/Al₂O₃ composites: Investigation of microstructure and mechanical properties [J]. *Materials and Design*, 2016, 109: 57–67.
- [26] HUANG Xiao-jian, YANG Jian-qiao, WEI Lang-lang, ZHANG Qiao-qiao, SHANG Wen-tao, LI Xu-jiao. Semi-solid microstructure evolution of Mg–7Zn–0.3Mn–xCu alloy [J]. *Transactions of Nonferrous Metals Society of China*, 2020, 30(6): 1238–1248.
- [27] KEIKO N, HIROSHI U, TATSUYA T. Improvement in formability of semi-solid cast hypoeutectic Al–Si alloys by equal-channel angular pressing [J]. *Journal of Materials Processing Technology*, 2017, 240: 240–248.
- [28] KANNO M, ARAKI I, CUI Q. Precipitation behaviour of

- 7000 alloys during retrogression and reaging treatment [J]. Materials Science and Technology, 1994, 10(7): 599–603.
- [29] CONSERVA M, RUSSO E, CALONI O. Comparison of the influence of chromium and zirconium on the quench sensitivity of Al–Zn–Mg–Cu alloys [J]. Metallurgical Transactions, 1971, 2(4): 1227–1232.
- [30] LIM S T, YUN S J, NAM S W. Improved quench sensitivity in modified aluminum alloy 7175 for thick forging applications [J]. Materials Science and Engineering A, 2004, 371: 82–90.

7075 铝合金在复杂触变挤压过程中的显微组织和力学性能

刘 健¹, 程远胜¹, Sin Wing Norman CHAN², Daniel SUNG²

1. 哈尔滨工业大学 金属精密热加工国家重点实验室, 哈尔滨 150001;
2. 嘉瑞科技有限公司, 惠州 516000

摘 要: 采用复杂触变挤压技术制备 7075 铝合金弯头零件, 随后采用 SEM、TEM 等分析方法研究材料在复杂触变挤压过程中显微组织和力学性能的变化。研究表明: 7075 铝合金弯头各部分的显微组织存在较大差异。反向挤压形成的薄壁部位的显微组织出现分层现象, 而角挤压形成的零件底部表现为明显的变形组织, 且剪切力可以促进晶粒和粗大第二相的破碎。材料中主要的强化相为 η 相和 E 相。在坯料加热至半固态和触变挤压的过程中, η 相和 E 相会大量减少。经过热处理后 η 相和 E 相均匀析出, 可提高材料的力学性能。经过触变挤压和热处理后, 弯头零件的平均抗拉强度为 485.49 MPa, 平均伸长率为 5.49%。

关键词: 7075 铝合金; 触变挤压; 半固态成形; 弯头零件; 力学性能

(Edited by Bing YANG)